Quadrature Channel Modulation

Ibrahim Yildirim, *Student Member, IEEE*, Ertugrul Basar, *Senior Member, IEEE*, and Ibrahim Altunbas, *Member, IEEE*

***Abstract*—In this letter, we propose the concept of quadrature channel modulation (QCM) by combining quadrature spatial modulation (QSM) and media-based modulation (MBM) transmission principles. The proposed QCM schemes exploit not only the in-phase and quadrature components of complex data symbols for antenna indexing but also channel states for the transmission of additional information bits through index modulation by employing a single radio frequency (RF) chain. It is shown via numerical studies that the proposed QCM schemes can outperform the existing emerging schemes such as QSM, plain MBM, and spatial modulation-based MBM, which also employ a single RF chain at their transmitters.**

***Index Terms*—Channel modulation, index modulation, media-based modulation, quadrature spatial modulation.**

I. Introduction

INDEX modulation (IM) provides new dimensions for the transmission of digital information and can be implemented by considering the indices of the transmit antennas (TAs) of a multiple-input multiple-output (MIMO) system [1], the subcarriers of an orthogonal frequency division multiplexing system [2] or the radio frequency (RF) mirrors of a reconfigurable antenna (RA) [3]. An RF mirror is an RA element that contains a PIN diode, which can be turned on or off according to the information bits to alter the radiation pattern of an RA [4], [5]. Some initial studies have been also performed for the practical realization of RAs with RF mirrors. As an example, Ourir *et al.* [6] implemented a compact RA with two RF mirrors and showed the corresponding radiation patterns, each of which leads to a different fading channel realization. Due to their attractive advantages such as improved energy/spectral efficiency, better error performance and lower complexity detection, over traditional digital modulation schemes [7], IM techniques have attracted remarkable attention in the past few years [8].

Although RAs with parasitic elements that are capable of altering their radiation patterns, are well-known in the field of electromagnetics; the concept of media-based modulation (MBM), which is one of the newest members of the vast IM family, has been proposed explicitly for the utilization of RAs to carry digital information [3], [9]. To resolve this ambiguity, the more general term of *channel modulation (CM)* has been recently introduced in [10] for the family of MBM/RA systems, which are actually based on the same concepts. In both systems (also in space-shift keying (SSK) that considers transmit antenna indices for IM), a carrier signal with constant parameters is transmitted while the realizations of the wireless channel convey information, i.e., the modulation of the wireless channel itself is performed from the perspective of the receiver. It has been also proved in [10] that MBM and SSK schemes are identical for specific system parameters.

The recent study of [11] considered the combination of generalized SM (GSM) techniques with MBM. It has been shown that due to additional information bits transmitted by antenna indices, GSM-MBM can achieve a better error performance than MIMO-MBM. A dual-polarized SM scheme, which considers the dimension of polarization for the transmission of an additional one information bit, is proposed in [12] for correlated Rayleigh and Rician fading channels. More recently, multidimensional IM concept is introduced in [13], where both RF mirrors, transmit antennas and time slots are considered for IM. SSK and MBM principles are also combined in [4] to improve the error performance of SSK considering correlated and nonidentically distributed Rician fading channels. Later, RA-based SSK [4] is considered for underlay cognitive radio systems in Rician fading channels and improvements are shown compared to conventional spectrum sharing systems [5]. Finally, the scheme space-time channel modulation (STCM) is introduced in [10] by combining space-time block coding and MBM concepts to further obtain transmit diversity gains. However, the design of high data rate SM-based CM schemes with single RF chain is still waiting to be explored.

In this letter, we introduce the concept of quadrature channel modulation (QCM) by combining quadrature SM (QSM) and MBM transmission principles to further improve the data rate of SM/SSK-based MBM (RA) schemes while ensuring simple implementation with a single RF chain. QSM appears as a promising SM variant with its high spectral efficiency and simple transceiver structure [14]. Our aim is to bring the attractive advantages of QSM, such as improved spectral efficiency and simple transceiver structure, into the field of CM by carefully designing a joint transmission mechanism, which outperforms both QSM and MBM schemes in terms of spectral efficiency and BER performance. Inspired by QSM, our scheme has three different operation modes that can provide interesting trade-offs among BER performance, data rate and complexity. Furthermore, our scheme can provide the same spectral efficiency as that of QSM by exploiting a considerably lower number of transmit antennas and only a single RF chain. It has been shown by theoretical average bit error rate (BER) derivations as well as comprehensive numerical studies that the proposed schemes can achieve better error performance than the reference single-input multiple-output (SIMO)-MBM, SM-MBM and conventional QSM schemes.

Manuscript received July 28, 2017; accepted August 17, 2017. Date of publication August 22, 2017; date of current version December 15, 2017. The associate editor coordinating the review of this paper and approving it for publication was V. Raghavan. *(Corresponding author: Ertugrul Basar.)*

The authors are with the Faculty of Electrical and Electronics Engineering, Istanbul Technical University, 34469 Istanbul, Turkey (e-mail: yildirimib@itu.edu.tr; basarer@itu.edu.tr; ibraltunbas@itu.edu.tr).

Digital Object Identifier 10.1109/LWC.2017.2742508

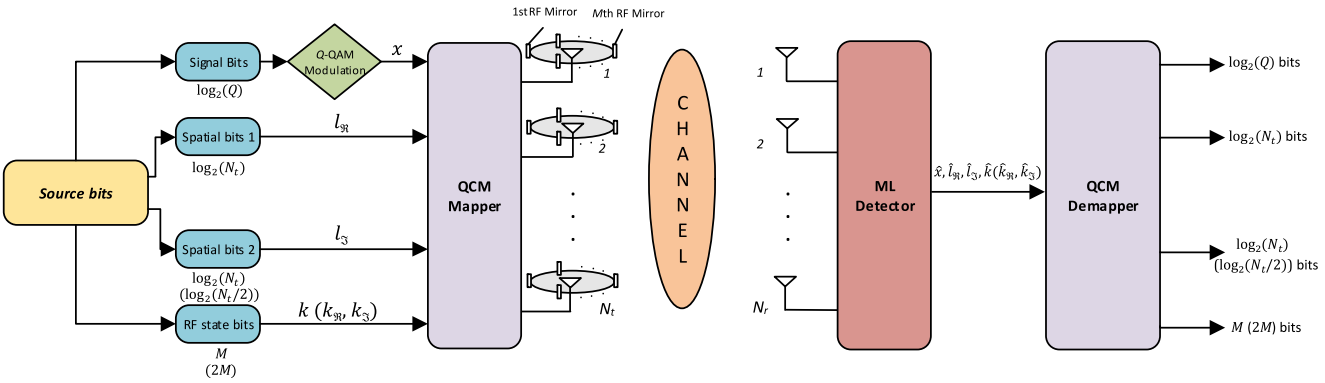

Fig. 1. Block diagram of the QCM-I/II schemes for an $N_r \times N_t$ MIMO system (The terms in parentheses are valid for the QCM-II scheme).

II. Quadrature Channel Modulation

In this section, we introduce the concept of QCM as well as provide design examples. Three novel QCM schemes are proposed by considering a MIMO system with N_r receive and N_t transmit antennas that employs Q-ary quadrature amplitude modulation (Q-QAM). Furthermore, each TA is equipped with M RF mirrors, which are used to create different channel realizations according to the information bits.

i) QCM-I Scheme: The system model of the QCM-I scheme is shown in Fig. 1. As seen from Fig. 1, this scheme is obtained by the direct combination of QSM and MBM principles. A total of

$$\eta = \log_2(Q) + 2\log_2(N_t) + M \tag{1}$$

bits enter the transmitter of the QCM-I scheme per channel use. Similar to the QSM scheme, the first $\log_2(Q)$ bits of the incoming bit sequence are used for ordinary Q-QAM, while the subsequent $2\log_2(N_t)$ bits select the indices ($l_\Re$ and $l_\Im$) of TAs for the transmission of in-phase and quadrature components of the selected Q-QAM symbol x. However, the last M bits are reserved for the selection of the active channel state (k), which is the same for all possible activated TAs of the QCM-I scheme. In other words, the QCM-I scheme extends the ordinary QSM into a third dimension, which is the dimension of channel states, to transmit additional information bits. In the following, we give an example for the operation of the QCM-I scheme.

Example 1: We consider the following system parameters: $N_t = N_r = 4$, $Q = 16$, $M = 2$ and $\eta = 10$ bits per channel use (bpcu). Assume that the input bits are grouped as follows:

$$\mathbf{q} = [\underbrace{1\ 0\ 0\ 1}_{\log_2(Q)}\ \underbrace{1\ 1}_{\log_2(N_t)}\ \underbrace{1\ 0}_{\log_2(N_t)}\ \underbrace{0\ 1}_{M}\ ]. \tag{2}$$

The first $\log_2(Q) = 4$ bits ($\begin{bmatrix}1 & 0 & 0 & 1\end{bmatrix}$) are modulated to obtain the 16-QAM symbol $x = 3 + j$. This data symbol is partitioned into its real and imaginary components as $x_\Re = +3$ and $x_\Im = +1$. Then, the next $\log_2(N_t) = 2$ bits ($\begin{bmatrix}1 & 1\end{bmatrix}$) determine the antenna index $l_\Re = 4$ over which the real component $x_\Re$ will be transmitted. Similarly, the following $\log_2(N_t) = 2$ bits ($\begin{bmatrix}1 & 0\end{bmatrix}$) select the antenna index $l_\Im = 3$ over which the imaginary component $x_\Im$ will be transmitted. Finally, the last M bits select the second channel state ($k = 2$), which corresponds to the following on/off status of the available RF mirrors for both activated TAs: 1st RF mirror $\rightarrow$ off and 2nd RF mirror $\rightarrow$ on.

ii) QCM-II Scheme: This scheme is proposed to further improve the spectral efficiency of the QCM-I scheme by ensuring that the real and imaginary components of the complex data symbols are not only transmitted from different TAs but also with two independent channel state realizations, which doubles the number of RF mirror bits. In order to perform two independent channel state selections ($k_\Re$ and $k_\Im$) for the QCM-II scheme, first, the set of available TAs is split in half into two groups and an antenna index $l_\Re$ is selected for $x_\Re$ from all available TAs without considering these groups. However, to activate a different antenna and perform a second channel state selection for $x_\Im$, the group associated with $l_\Re$ is not considered for $l_\Im$. The reason for this adaptive selection is to transmit more number of IM bits via TA indices as seen from Fig. 1. As a result, the spectral efficiency of the QCM-II scheme becomes

$$\eta = \log_2(Q) + \log_2(N_t) + \log_2(N_t/2) + 2M \quad \text{bpcu}. \tag{3}$$

iii) QCM-III Scheme: This QCM scheme is inspired from the QCM-I scheme; however, it owns a reserved TA as in [15], which is employed instead of the selected TA of $x_\Re$ to independently perform active channel state selection for $x_\Re$ and $x_\Im$, similar to the QCM-II scheme. On the other hand, due to the utilization of a reserved TA, there is no need for TA partitioning as in the QCM-II scheme, and a higher spectral efficiency can be obtained by considering two parallel virtual SM-MBM schemes for both $x_\Re$ and $x_\Im$ as shown in Fig. 2. Consequently, the spectral efficiency of this scheme becomes

$$\eta = \log_2(Q) + 2\log_2(N_t) + 2M \quad \text{bpcu}. \tag{4}$$

Example 2: We consider the following system parameters: $N_t = 4$, a reserved TA, $N_r = 4$, $Q = 4$, $M = 2$ and $\eta = 10$ bpcu. Assume that the input bits are grouped as follows:

$$\mathbf{q} = [\underbrace{1\ 1}_{\log_2(Q)}\ \underbrace{1\ 0}_{\log_2(N_t)}\ \underbrace{1\ 0}_{\log_2(N_t)}\ \underbrace{0\ 1}_{M}\ \underbrace{1\ 1}_{M}\ ]. \tag{5}$$

The first $\log_2(Q) = 2$ bits ($\begin{bmatrix}1 & 1\end{bmatrix}$) are modulated to obtain the 4-QAM symbol $x = 1 - j$, which is decomposed into its real and imaginary components as $x_\Re = 1$ and $x_\Im = -1$. Then, the subsequent $\log_2(N_t) = 2$ bits ($\begin{bmatrix}1 & 0\end{bmatrix}$) determine the antenna index $l_\Re = 3$ over which the real component $x_\Re$ will be transmitted. For $x_\Im$, the reserved TA is employed

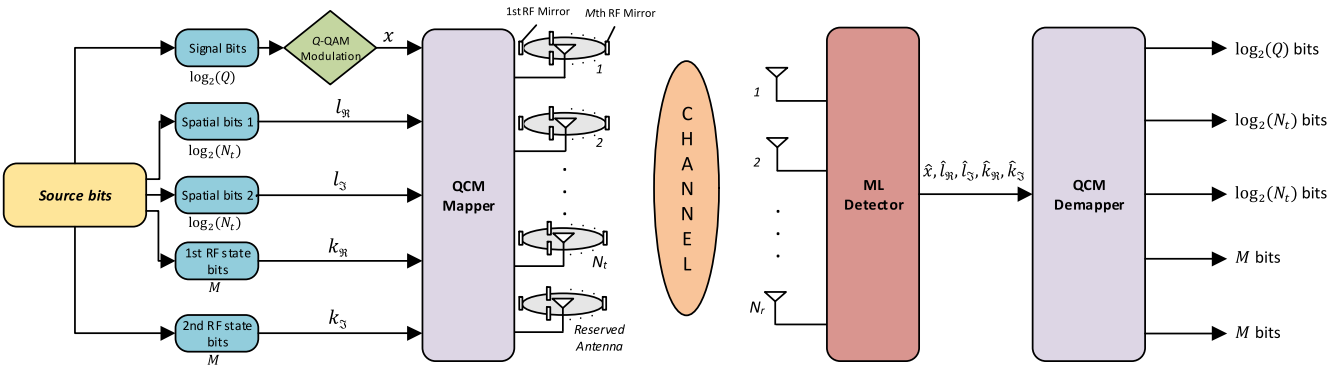

Fig. 2. Block Diagram of the QCM-III scheme for an $N_r \times (N_t + 1)$ MIMO system.

instead of the previously selected TA for $x_{\Re}$, and the next $\log_2(N_t) = 2$ bits ($[1 \quad 0]$) select $l_{\Im} = 4$ from the available TA set $\{1, 2, 4, 5\}$ since the third antenna has already reserved. Finally, the remaining $2M = 4$ bits can select two independent channel states, which are $k_{\Re} = 2$ and $k_{\Im} = 4$, for the two activated TAs $l_{\Re} = 3$ and $l_{\Im} = 4$, respectively.

The baseband signal model of the QCM scheme can be expressed as

$$\mathbf{y} = \mathbf{H}\mathbf{s} + \mathbf{n} \tag{6}$$

where $\mathbf{y} \in \mathbb{C}^{N_r \times 1}$ and $\mathbf{n} \in \mathbb{C}^{N_r \times 1}$ are vectors of the received signals and noise samples, respectively. $\mathbf{H}$ and $\mathbf{s}$ respectively stand for the extended channel matrix and transmission vector of the QCM scheme. For QCM-I/II schemes, their dimensions are $N_r \times 2^M N_t$ and $2^M N_t \times 1$, respectively, while the corresponding dimensions for the QCM-III scheme are $N_r \times 2^M(N_t + 1)$ and $2^M(N_t + 1) \times 1$. We assume that the elements of $\mathbf{H}$ and $\mathbf{n}$ follow $\mathcal{CN}(0, 1)$ and $\mathcal{CN}(0, N_0)$ distributions, respectively. The general form of $\mathbf{s}$ is given as

$$\mathbf{s} = [\ \cdots\ \vdots\ 0 \cdots \overbrace{x_{\Re}}^{l_{\Re}} \cdots 0 \ \vdots\ \cdots\ \vdots\ 0 \cdots \overbrace{jx_{\Im}}^{l_{\Im}} \cdots 0 \ \vdots \cdots\ ]^T \tag{7}$$
$$\text{Ch. State } k_{\Re} \qquad \text{Ch. State } k_{\Im}$$

where for the QCM-I scheme, $k_{\Re} = k_{\Im} = k$, while $k_{\Re}$ and $k_{\Im}$ are independently selected for QCM-II/III schemes. It should be noted that only one or two elements of $\mathbf{s}$ are non-zero. Furthermore, QCM-II/III schemes also ensure that $l_{\Re} \neq l_{\Im}$ to enable independent channel state selections for $x_{\Re}$ and $x_{\Im}$. For the above two examples, the corresponding transmission vectors are respectively given as follows:

$$\mathbf{s} = [\ \underbrace{0000}_{\text{Ch. State 1}}\ \vdots\ \underbrace{00\ \overbrace{j}^{l_{\Im}}\ \overbrace{3}^{l_{\Re}}}_{\text{Ch. State 2}}\ \vdots\ \underbrace{0000}_{\text{Ch. State 3}}\ \vdots\ \underbrace{0000}_{\text{Ch. State 4}}\ ]^T,$$
$$\mathbf{s} = [\ \underbrace{00000}_{\text{Ch. State 1}}\ \vdots\ \underbrace{00\ \overbrace{1}^{l_{\Re}}\ 00}_{\text{Ch. State 2}}\ \vdots\ \underbrace{00000}_{\text{Ch. State 3}}\ \vdots\ \underbrace{000\ \overbrace{-j}^{l_{\Im}}\ 0}_{\text{Ch. State 4}}\ ]^T. \tag{8}$$

Similarly, the transmission vector for the QCM-II scheme can be easily obtained.

The maximum-likelihood (ML) detection for QCM schemes can be performed by the following exhaustive search:

$$[\hat{x}, \hat{l}_{\Re}, \hat{l}_{\Im}, \hat{k}_{\Re}, \hat{k}_{\Im}] = \arg \min_{x, l_{\Re}, l_{\Im}, k_{\Re}, k_{\Im}} \|\mathbf{y} - \mathbf{H}\mathbf{s}\|^2 \tag{9}$$

where $\|.\|$ stands for the Euclidean norm.

III. Theoretical Analysis of QCM

In this section, theoretical average BER of QCM is evaluated considering the system model of (6). If $\mathbf{s}$ is transmitted and it is erroneously detected as $\hat{\mathbf{s}}$, the corresponding conditional pairwise error probability (PEP) is given by [10]

$$P(\mathbf{s} \to \hat{\mathbf{s}}|\mathbf{H}) = P(\|\mathbf{y} - \mathbf{H}\mathbf{s}\|^2 > \|\mathbf{y} - \mathbf{H}\hat{\mathbf{s}}\|^2) = Q\left(\sqrt{\frac{\Delta}{2N_0}}\right) \tag{10}$$

where $\Delta = \|\mathbf{H}(\mathbf{s} - \hat{\mathbf{s}})\|^2$. Using the alternative form of the Q-function and moment generating function [16] of Δ, given by $M_{\Delta}(t) = (1 - t\|\mathbf{s} - \hat{\mathbf{s}}\|^2)^{-N_r}$, the unconditional PEP is obtained as

$$P(\mathbf{s} \to \hat{\mathbf{s}}) = \frac{1}{\pi} \int_0^{\frac{\pi}{2}} \left(\frac{\sin^2\theta}{\sin^2\theta + \frac{\|\mathbf{s} - \hat{\mathbf{s}}\|^2}{4N_0}} \right)^{N_r} d\theta \tag{11}$$

which has a closed form solution in [16]. After the derivation of unconditional PEP, the average BER upper bound of QCM can be obtained with $P_b \approx \frac{1}{\eta 2^{\eta}} \sum_{\mathbf{s}} \sum_{\hat{\mathbf{s}}} P(\mathbf{s} \to \hat{\mathbf{s}})\, e(\mathbf{s}, \hat{\mathbf{s}})$, where $e(\mathbf{s}, \hat{\mathbf{s}})$ stands for the number of bit errors for the pairwise error event of $(\mathbf{s} \to \hat{\mathbf{s}})$.

IV. Numerical Studies

In this section, we provide computer simulation results for the proposed QCM schemes and make comparisons with the classical QSM [14], SIMO-MBM [3] and SM-MBM [11] schemes with respect to E_b/N_0, where E_b is the average transmitted energy per bit. We consider natural mapping for channel states and TA indices, while we employ Gray mapping for M-PSK/QAM symbols.

In Fig. 3, the theoretical average BER upper bounds of the QCM-I scheme are compared with computer simulation results for different spectral efficiency values, while similar results can be easily obtained for the QCM-II/III schemes. As seen from Fig. 3, the derived theoretical average BER

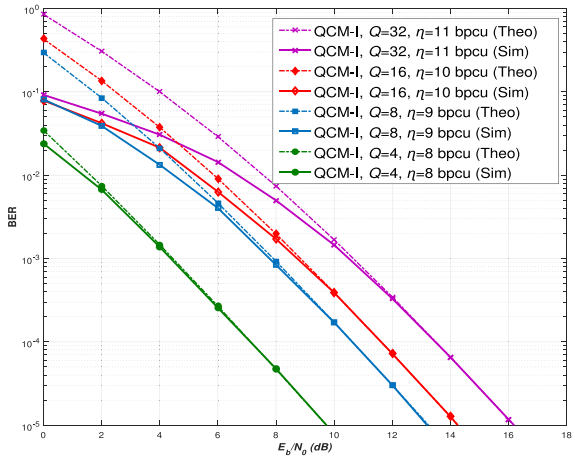

Fig. 3. Theoretical average BER of the QCM-I scheme with four transmit and receive antennas and two RF mirrors with different bpcu values.

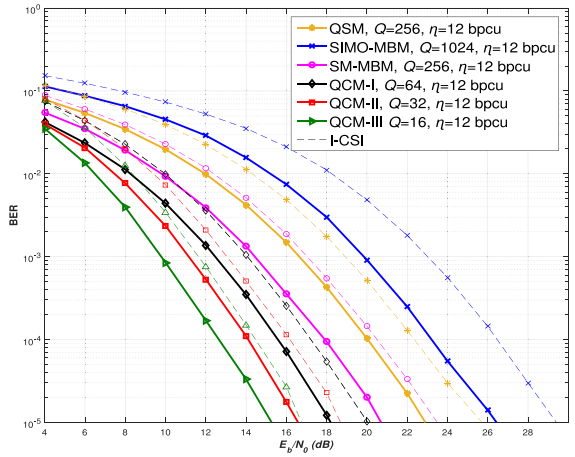

Fig. 4. BER performance of QCM and reference systems with four transmit and receive antennas, two RF mirrors and $\eta = 12$, (I-CSI: imperfect CSI).

upper bounds accurately predict the BER performance of the proposed scheme.

In Fig. 4, we provide BER performance curves of the proposed QCM schemes and make comparisons with the reference systems for $\eta = 12$ bpcu. As seen from Fig. 4, all three proposed QCM schemes achieve considerably better BER performance than the reference QSM, SIMO-MBM and SM-MBM schemes, which also employ a single RF chain at their transmitters. The reason for this BER performance improvement can be explained by the fact that the reference MBM and QSM schemes need to employ higher order constellations to reach the same spectral efficiency as that of QCM schemes. Similarly, the proposed schemes can achieve a higher spectral efficiency than the reference systems for the same modulation order since the proposed schemes employ a more effective IM mechanism. It is interesting to note that QCM-III scheme achieves the best BER performance by using an additional reserved TA. On the other hand, the QCM-II scheme provides a satisfactory BER performance and outperforms the QCM-I scheme with a more complicated mapping rule. In Fig. 4, we also investigate the performance of the proposed as well as reference systems in the presence of channel estimation errors. For the imperfect channel state information (I-CSI) case, the channel matrix at the receiver is obtained as $\hat{\mathbf{H}} = \mathbf{H} + \mathbf{E}$, where the elements of $\mathbf{E}$ follow $\mathcal{CN}(0, \sigma_\epsilon^2)$ distribution. It is assumed that the power of channel estimation errors is related with N_0 as $\psi = N_0/\sigma_\epsilon^2$. As seen from Fig. 4, the proposed schemes are also robust to channel estimation errors as the reference systems for $\psi = 1$.

V. Conclusion

In this letter, we have proposed the concept of QCM to improve the data rate of plain MBM and QSM schemes by exploiting both channel states and in-phase/quadrature components of the complex data symbols for data transmission through IM. We have shown by extensive numerical studies and theoretical derivations that the proposed QCM schemes with single RF chain outperform the classical QSM and existing MBM-based systems. The design of low-complexity detectors for the proposed QCM schemes, due to the sparsity of their transmission vectors, can be considered as our future work.

References

[1] P. Yang, M. Di Renzo, Y. Xiao, S. Li, and L. Hanzo, "Design guidelines for spatial modulation," *IEEE Commun. Surveys Tuts.*, vol. 17, no. 1, pp. 6–26, 1st Quart., 2015.

[2] E. Basar, U. Aygölü, E. Panayirci, and H. V. Poor, "Orthogonal frequency division multiplexing with index modulation," *IEEE Trans. Signal Process.*, vol. 61, no. 22, pp. 5536–5549, Nov. 2013.

[3] A. K. Khandani, "Media-based modulation: Converting static Rayleigh fading to AWGN," in *Proc. IEEE Int. Symp. Inf. Theory*, Honolulu, HI, USA, Jun. 2014, pp. 1549–1553.

[4] Z. Bouida, H. El-Sallabi, A. Ghrayeb, and K. A. Qaraqe, "Reconfigurable antenna-based space-shift keying (SSK) for MIMO Rician channels," *IEEE Trans. Wireless Commun.*, vol. 15, no. 1, pp. 446–457, Jan. 2016.

[5] Z. Bouida, H. El-Sallabi, M. Abdallah, A. Ghrayeb, and K. A. Qaraqe, "Reconfigurable antenna-based space-shift keying for spectrum sharing systems under Rician fading," *IEEE Trans. Commun.*, vol. 64, no. 9, pp. 3970–3980, Sep. 2016.

[6] A. Ourir, K. Rachedi, D.-T. Phan-Huy, C. Leray, and J. de Rosny, "Compact reconfigurable antenna with radiation pattern diversity for spatial modulation," in *Proc. 11th Eur. Conf. Antennas Propag.*, Paris, France, Mar. 2017, pp. 3038–3043.

[7] R. Rajashekar, K. V. S. Hari, and L. Hanzo, "Reduced-complexity ML detection and capacity-optimized training for spatial modulation systems," *IEEE Trans. Commun.*, vol. 62, no. 1, pp. 112–125, Jan. 2014.

[8] E. Basar, "Index modulation techniques for 5G wireless networks," *IEEE Commun. Mag.*, vol. 54, no. 7, pp. 168–175, Jul. 2016.

[9] E. Seifi, M. Atamanesh, and A. K. Khandani. (Oct. 2015). *Media-Based MIMO: A New Frontier in Wireless Communication*. [Online]. Available: http://arxiv.org/abs/1507.07516

[10] E. Basar and I. Altunbas, "Space-time channel modulation," *IEEE Trans. Veh. Technol.*, vol. 66, no. 8, pp. 7609–7614, Aug. 2017.

[11] Y. Naresh and A. Chockalingam, "On media-based modulation using RF mirrors," *IEEE Trans. Veh. Technol.*, vol. 66, no. 6, pp. 4967–4983, Jun. 2017.

[12] G. Zafari, M. Koca, and H. Sari, "Dual-polarized spatial modulation over correlated fading channels," *IEEE Trans. Commun.*, vol. 65, no. 3, pp. 1336–1352, Mar. 2017.

[13] B. Shamasundar, S. Jacob, S. Bhat, and A. Chockalingam, "Multidimensional index modulation in wireless communications," in *Proc. Inf. Theory Appl. Workshop*, San Diego, CA, USA, Feb. 2017, pp. 1–10. [Online]. Available: https://arxiv.org/abs/1702.03250

[14] R. Mesleh, S. S. Ikki, and H. M. Aggoune, "Quadrature spatial modulation," *IEEE Trans. Veh. Technol.*, vol. 64, no. 6, pp. 2738–2742, Jun. 2015.

[15] S. Fang *et al.*, "Layered space shift keying modulation over MIMO channels," *IEEE Trans. Veh. Technol.*, vol. 66, no. 1, pp. 159–174, Jan. 2017.

[16] M. Simon and M. S. Alaouni, *Digital Communications Over Fading Channels*. New York, NY, USA: Wiley, 2005.